pH-Dependent Investigations of Vanadium(V)−Peroxo−Malate Complexes from Aqueous Solutions. In Search of Biologically Relevant Vanadium(V)−Peroxo Species

M. Kaliva, T. Giannadaki, and A. Salifoglou*

Department of Chemistry, University of Crete, Heraklion 71409, Greece

C. P. Raptopoulou and A. Terzis

Institute of Materials Science, NCSR "Demokritos", Aghia Paraskevi 15310, Attiki, Greece

V. Tangoulis

Department of Materials Science, University of Patras, Patras 26500, Greece

Received August 7, 2000

The established biochemical potential of vanadium has spurred considerable research interest in our lab, with specific focus on pertinent synthetic studies of vanadium(III) with a biologically relevant, organic, dicarboxylic acid, malic acid, in aqueous solutions. Simple reactions between VCl_3 and malic acid in water, at different pH values, in the presence of H_2O_2, led to the crystalline dimeric complexes $(Cat)_4[VO(O_2)(C_4H_3O_5)]_2 \cdot nH_2O$ (Cat = K^+, $n = 4$, **1**; Cat = NH_4^+, $n = 3$, **2**) and $K_2[VO(O_2)(C_4H_4O_5)]_2 \cdot 2H_2O$ (**3**). All three complexes were characterized by elemental analysis, FT-IR, and UV/visible spectroscopies. Compound **1** crystallizes in the monoclinic space group $P2_1/c$, with $a = 8.380(5)$ Å, $b = 9.252(5)$ Å, $c = 13.714(8)$ Å, $\beta = 93.60(2)°$, $V = 1061(1)$ Å^3, and $Z = 4$. Compound **2** crystallizes in the triclinic space group $P\bar{1}$, with $a = 9.158(4)$ Å, $b = 9.669(4)$ Å, $c = 14.185(6)$ Å, $\alpha = 104.81(1)°$, $\beta = 90.31(1)°$, $\gamma = 115.643(13)°$, $V = 1085.0(7)$ Å^3, and $Z = 2$. Compound **3** crystallizes in the monoclinic space group $P2_1/c$, with $a = 9.123(8)$ Å, $b = 9.439(8)$ Å, $c = 10.640(9)$ Å, $\beta = 104.58(3)°$, $V = 887(1)$ Å^3, and $Z = 2$. The X-ray structures showed that, in **1** and **2,** the dimers consist of two $(V^V{=}O)_2O_2$ rhombic units to which two malate ligands are attached. The ligands are triply deprotonated and, as such, they coordinate to vanadium(V), promoting a pentagonal bipyramidal geometry. In **3**, the dimeric $(V^V{=}O)_2O_2$ rhombic unit persists, with the two doubly deprotonated malate ligands coordinated to the vanadium(V) ions. UV/vis and EPR spectroscopic studies on the intermediate blue solutions of the synthesis reactions of **1**−**3** support the existence of vanadyl-containing dimeric species. These species further react with H_2O_2 to yield oxidation of $V^{IV}{}_2O_2$ to $V^V{}_2O_2$ and coordination of the peroxide to vanadium(V). From the collective data on **1**−**3,** it appears that pH acts as a decisive factor in dictating the structural features of the isolated complexes. The details of the introduced structural differentiation in the reported complexes, and their potential relevance to vanadium(V) dicarboxylate systems in biological media are dwelled on.

Introduction

Vanadium chemistry has increasingly become the center of research attention, as its involvement in biological systems has emerged as essential in recent years.[1] Vanadium, an element with diverse chemical properties, has been found in metalloenzyme systems, participating in active site metallocenters,[2] conferring specific functions upon them, and influencing their catalytic reactivity. Among such biosystems, known to date, are alternative nitrogenases,[3] haloperoxidases,[4] and others.[5] Recent discoveries, however, have brought to light the unique properties of vanadium originating from its broader interaction with living systems. Such properties bring about enzyme inhibitory,[6] mitogenic,[7] antitumorigenic,[8] and insulinomimetic

* To whom correspondence should be addressed. Tel: +30-81-393-652. Fax: +30-81-393-601. E-mail: salif@chemistry.uoc.gr.

(1) Wever, R.; Kustin, K. In *Advances in Inorganic Chemistry: Vanadium, a Biologically Relevant Element*; Sykes, A. G., Ed.; Academic Press: New York, 1990; Vol. 35, pp 103−137.
(2) Rehder, D. *Biometals* **1992**, *5*, 3−12.
(3) Liang, J.; Madden, M.; Shah, V. K.; Burris, R. H. *Biochemistry* **1990**, *29*, 8577−8581.
(4) (a) Weyand, M.; Hecht, H.; Kiess, M.; Liaud, M.; Vilter, H.; Schomburg, D. *J. Mol. Biol.* **1999**, *293*, 595−611. (b) Vilter, H. In *Metal Ions in Biological Systems: Vanadium and its Role in Life*; Sigel, H., Sigel, A., Eds.; Marcel Dekker: New York, 1995; Vol. 31, Chapter 10, pp 325−362. (c) Butler, A. *Curr. Opin. Chem. Biol.* **1998**, *2*, 279−285.
(5) (a) Bayer, E. In *Metal Ions in Biological Systems: Amavadin, the Vanadium Compound of Amanitae*; Sigel, H., Sigel, A., Eds.; Marcel Dekker: New York, 1995; Vol. 31, Chapter 12, pp 407−421. (b) Smith, M. J.; Ryan, D. E.; Nakanishi, K.; Frank, P.; Hodgson, K. O. In *Metal Ions in Biological Systems: Vanadium in Ascidians and the Chemistry in Tunichromes*; Sigel, H., Sigel, A., Eds.; Marcel Dekker: New York, 1995; Vol. 31, Chapter 13, pp 423−490. (c) Frausto da Silva, J. J. R. *Chemical Speciation Bioavailability*, **1989**, *1*, 139−150.
(6) (a) Walton, K. M.; Dixon, J. E. *Annu. Rev. Biochem.* **1993**, *62*, 101−120. (b) Lau, K.-H. W.; Farley, J. R.; Baylink, D. J. *Biochem. J.* **1989**, *257*, 23−36.
(7) (a) Klarlund, J. K. *Cell* **1985**, *41*, 707−717. (b) Smith, J. B. *Proc. Natl. Acad. Sci. U.S.A.* **1983**, *80*, 6162−6167.

10.1021/ic000894o CCC: $20.00
Published on Web 06/19/2001

activities.[9] Key to a number of such metabolic actions appears to be the basic chemical interactions of that metal ion with large and small molecules in biological media. Species resulting from such interactions include, among others, vanadium−peroxo complexes.[10] Carboxylic acids have been known to exist in biological media and to influence strategic metabolic pathways, governing the physiological activities of cells and multicellular organisms. Malic acid is one of the dicarboxylic acids present in human plasma and is heavily involved in the citric acid cycle.[11] It is with acids, like malic acid, that vanadium ions could forge interactions and form peroxo complexes, in synergy with hydrogen peroxide, which might bear relevance to diverse biological activities.[8,10a,12]

Despite the intense biological work carried out so far,[13] suggesting possible modes of action of vanadium at different oxidation states (V^V and V^{IV}) in biological media, fundamental structural information pertaining to well-characterized vanadium−peroxo species with physiologically relevant dicarboxylate ligands—such as malate—in aqueous solutions is limited. The need to discover such new species, potentially useful in delineating the role of vanadium in biofluids, has attracted our attention. To that end, we pursued the development of the pH-dependent aqueous synthetic oxidative chemistry of vanadium(III) with dicarboxylic acids and hydrogen peroxide, being aware of (a) the potential complexity of ternary vanadium(V)−peroxo−dicarboxylate ligand interactions, (b) the diverse coordination chemistry of vanadium(V) expected in the presence of coordinatively versatile dicarboxylate ligands in aqueous solutions, and (c) the rich information it could provide on the biodistribution of that metal, in the 5+ oxidation state, present in biological media. Having chosen malic acid as a representative dicarboxylic moiety of biological relevance, we report herein the synthesis, isolation, structural studies, and spectroscopic characterization of new vanadium(V)−malate−peroxo complexes, as a function of the pH of the aqueous solution in which their synthesis is pursued.

(8) Djordjevic, C. In *Metal Ions in Biological Systems: Antitumorigenic Activity of Vanadium Compounds*; Sigel, H., Sigel, A., Eds.; Marcel Dekker: New York, 1995; Vol. 31, Chapter 18, pp 595−616.

(9) (a) Brand, R. M.; Hamel, F. G. *Int. J. Pharm.* **1999,** *183*, 117−123. (b) Drake, P. G.; Posner, B. I. *Mol. Cell Biochem.* **1998**, *182*, 79−89. (c) Drake, P. G.; Bevan, A. P.; Burgess, J. W.; Bergeron, J. J.; Posner, B. I. *Endocrinology* **1996**, *137*, 4960−4968. (d) Eriksson, J. W.; Lonnroth, P.; Posner, B. I.; Shaver, A.; Wesslau, C.; Smith, U. P. *Diabetologia* **1996**, *39*, 235−242. (e) Stankiewicz, P. J.; Tracey, A. S. O. In *Metal Ions in Biological Systems: Stimulation of Enzyme Activity by Oxovanadium Complexes*; Sigel, H., Sigel, A., Eds.; Marcel Dekker: New York, 1995; Vol. 31, Chapter 8, pp 249−285.

(10) (a) Shaver, A.; Ng, J. B.; Hall, D. A.; Loon, B. S.; Posner, B. I. *Inorg. Chem.* **1993**, *32*, 3109. (b) Jaswal, J. S.; Tracey, A. S. *Inorg. Chem.* **1991**, *30*, 3718−3722. (c) Harrison, A. T.; Howarth O. W. *J. Chem. Soc., Dalton Trans.* **1985**, 1173−1177. (d) Stomberg, R.; Olson, S.; Swenson, I.-B. *Acta Chem. Scand.* **1984**, *A38*, 653.

(11) (a) Crans, D. C. In *Metal Ions in Biological Systems: Vanadium and its Role in Life*; Sigel, H., Sigel, A., Eds.; Marcel Dekker: New York, 1995; Vol. 31, Chapter 5, pp 147−209. (b) Martin, R. B. *J. Inorg. Biochem.* **1986**, *28*, 181−187.

(12) (a) Djordjevic, C.; Vuletic, N.; Renslo, M. L.; Puryear, B. C.; Alimard, R. *Mol. Cell. Biochem.* **1995**, *153*, 25−29. (b) Posner, B. I.; Faure, R.; Burgess, J. W.; Bevan, A. P.; Lachance, D.; Zhang-Sun, G.; Fantus, I. G.; Ng, J. B.; Hall, D. A.; Soo Lum, B.; Shaver, A. *J. Biol. Chem.* **1994**, *269*, 4596−4604. (c) Shisheva, A.; Shechter, Y. *Endocrinology*, **1993**, *133*, 1562−1568. (d) Kadota, S.; Fantus, G.; Deragon, G.; Guyda, H. J.; Hersh, B.; Posner, B. I. *Biochem. Biophys. Res. Commun.* **1987**, *147*, 259−266.

(13) (a) Kiss, T.; Buglyo, P.; Sanna, D.; Micera, G.; Decock, P.; Dewaele, D. *Inorg. Chim. Acta* **1995**, *239*, 145−153. (b) Crans, D. C.; Ehde, P. M.; Shin, P. K.; Pettersson, L. *J. Am. Chem. Soc.* **1991**, *113*, 3728−3736. (c) Crans, D. C.; Felty, R. A.; Miller, M. M. *J. Am. Chem. Soc.* **1991**, *113*, 265−269. (d) Tracey, A. L.; Li, H.; Gresser, M. J. *Inorg. Chem.* **1990**, *29*, 2267−2271. (e) Crans, D. C.; Bunch, R. L.; Theisen, L. A. *J. Am. Chem. Soc.* **1989**, *111*, 7597−7607.

Experimental Section

Materials and Methods. All experiments were carried out in the open air. Nanopure quality water was used for all reactions. VCl_3, DL-malic acid, and H_2O_2 (30%) were purchased from Aldrich. KOH and ammonia were supplied by Fluka.

Physical Measurements. Electronic spectra were recorded on a Hitachi U-2001 UV/vis spectrophotometer in the range 200−1000 nm. FT-infrared measurements were taken on a Perkin-Elmer 1760X FT-infrared spectrometer. The EPR spectra of the intermediate blue solutions derived from reactions leading to **1** and **3** were recorded on a Bruker ER 200D-SRC X-band spectrometer, equipped with an Oxford ESR 9 cryostat at 9.174 GHz, 10dB, at room temperature and 4 K. Elemental analyses were performed by Quantitative Technologies, Inc.

Preparation of Complexes. (a) $K_4[V_2O_2(O_2)_2(C_4H_3O_5)_2]\cdot 4H_2O$ (1). VCl_3 (0.08 g, 0.51 mmol) and malic acid (0.068 g, 0.51 mmol) were placed in a flask and dissolved in 5 mL of H_2O. To the resulting light-blue reaction mixture was added 0.10 M KOH dropwise and under stirring, until the color of the solution became green and pH ∼8. Subsequently, the reaction mixture was stirred overnight. On the following day, the solution was blue and the pH was 6.5. The reaction flask was placed in an ice bath, and to it was added H_2O_2 (30%, 0.23 mL, 2.04 mmol) dropwise and under continuous stirring. The color of the reaction mixture became orange-red, and stirring continued for an additional 35 min. Subsequently, ethanol was added and the flask was placed in the refrigerator. One week later, red crystalline material precipitated, which was isolated by filtration and dried in vacuo. Yield: 0.08 g (50%). Anal. Calcd for **1**, $K_4[V_2O_2(O_2)_2(C_4H_3O_5)_2]\cdot 4H_2O$ ($C_8H_{14}O_{20}K_4V_2$, MW = 688.49): C, 13.94; H, 2.03; K, 22.66. Found: C, 14.02; H, 2.08; K, 22.89.

(b) $(NH_4)_4[V_2O_2(O_2)_2(C_4H_3O_5)_2]\cdot 3H_2O$ (2). VCl_3 (0.09 g, 0.57 mmol) and malic acid (0.08 g, 0.57 mmol) were dissolved in 5 mL of water. To that solution was added 0.1 M aqueous ammonia dropwise until pH ∼8, and the color of the solution became green. Subsequently, the reaction mixture was stirred overnight. On the following day, the solution was blue and pH ∼6. The reaction flask was then placed in an ice bath, and H_2O_2 (30%, 0.19 mL, 1.71 mmol) was added dropwise. The color of the solution turned orange, and stirring continued for an additional 35 min. Subsequently, ethanol was added and the reaction flask was placed at 4 °C. One week later, red crystals formed, which were isolated by filtration and dried in vacuo. Yield: 0.08 g (48%). Anal. Calcd for **2**, $(NH_4)_4[V_2O_2(O_2)_2(C_4H_3O_5)_2]\cdot 3H_2O$ ($C_8H_{28}O_{19}N_4V_2$, MW = 586.22): C, 16.39; H, 4.78; N, 9.56. Found: C, 16.41; H, 4.68; N, 9.46.

(c) $K_2[V_2O_2(O_2)_2(C_4H_4O_5)_2]\cdot 2H_2O$ (3). VCl_3 (0.09 g, 0.57 mmol) and malic acid (0.077 g, 0.57 mmol) were dissolved in 5 mL of H_2O. The pH of the resulting solution was adjusted to 6.5 with a 0.10 M solution of KOH, and the color of the solution turned green. The reaction mixture was stirred overnight. On the following day, the pH of the solution was ∼4.5, and the color had turned blue. The reaction flask was placed in an ice bath, and H_2O_2 (30%, 0.26 mL, 2.28 mmol) was added dropwise and under continuous stirring. The color of the reaction mixture changed to orange, and stirring continued for an additional 30 min. Subsequently, ethanol was added and the reaction flask was placed at 4 °C. A few days later, red crystalline material appeared, at the bottom of the flask, and was isolated by filtration followed by drying in vacuo. Yield: 0.07 g (43%). Anal. Calcd for **3**, $K_2[V_2O_2(O_2)_2(C_4H_4O_5)_2]\cdot 2H_2O$ ($C_8H_{12}O_{18}K_2V_2$, MW = 576.26): C, 16.67; H, 2.08; K, 13.54. Found: C, 16.11; H, 2.15; K, 13.48.

X-ray Crystallography. Crystal Structure Determination. X-ray-quality crystals of compounds **1**−**3** were grown from water−ethanol mixtures. Single crystals, with dimensions 0.10 × 0.25 × 0.50 mm (**1**) and 0.10 × 0.20 × 0.40 mm (**3**), were mounted on a Crystal Logic dual-goniometer diffractometer, using graphite-monochromated Mo Kα radiation. Crystals of compound **2**, with dimensions 0.10 × 0.10 × 0.40 mm, were examined on a $P2_1$ Nicolet diffractometer, using Ni-filtered Cu Kα radiation. Unit cell dimensions for **1** and **3** were determined and refined by using the angular settings of 25 automatically centered reflections in the range $11° < 2\theta < 23°$, while for **2** the angular settings of 25 automatically centered reflections in the range $24° < 2\theta < 54°$ were used. Relevant crystallographic details are given in Table

Table 1. Summary of Crystal, Intensity Collection, and Refinement Data for $K_4[V_2O_2(O_2)_2(C_4H_3O_5)_2]\cdot 4H_2O$ (**1**), $(NH_4)_4[V_2O_2(O_2)_2(C_4H_3O_5)_2]\cdot 3H_2O$ (**2**), and $K_2[V_2O_2(O_2)_2(C_4H_4O_5)_2]\cdot 2H_2O$ (**3**)

	1	**2**	**3**
formula	$C_8H_{14}K_4O_{20}V_2$	$C_8H_{28}N_4O_{19}V_2$	$C_8H_{12}K_2O_{18}V_2$
formula weight	688.49	586.22	576.26
T, °K	298	298	298
wavelength	Mo Kα 0.71073	Cu Kα 1.54180	Mo Kα 0.71073
space group	$P2_1/c$	$P\bar{1}$	$P2_1/c$
a, Å	8.380(5)	9.158(4)	9.123(8)
b, Å	9.252(5)	9.669(4)	9.439(8)
c, Å	13.714(8)	14.185(6)	10.640(9)
α, deg		104.81(1)	
β, deg	93.60(2)	90.31(1)	104.58(3)
γ, deg		115.643(13)	
V, Å^3	1061(1)	1085.0(7)	887(1)
Z	4	2	2
D_{calcd}/D_{obsd} (Mg m^{-3})	2.155/2.13	1.794/1.77	2.158/2.13
abs coeff (μ), mm^{-1}	1.762	8.149	1.620
range of *h*,*k*,*l*	$-9\rightarrow 9$, $-11\rightarrow 0$, $-16\rightarrow 0$	$-10\rightarrow 10$, $-11\rightarrow 10$, $0\rightarrow 16$	$-10\rightarrow 0$, $0\rightarrow 11$, $-12\rightarrow 12$
goodness-of-fit on F^2	1.040	1.068	1.096
R indices[d]	R1 = 0.0289, wR_2 = 0.0753[a]	R1 = 0.0498, wR2 = 0.1315[b]	R1 = 0.0280, wR2 = 0.0752[c]
R indices (all data)[d]	R1 = 0.0318, wR_2 = 0.0778	R1 = 0.0687, wR2 = 0.1756	R1 = 0.0302, wR2 = 0.0768

[a] 1999 refs; $I > 2\sigma(I)$. [b] 2730 refs; $I > 2\sigma(I)$. [c] 1462 refs; $I > 2\sigma(I)$. [d] $R1 = \sum||F_o| - |F_c||/\sum(|F_o|)$, $wR2 = \{\sum[w(F_o^2 - F_c^2)^2]/\sum[w(F_o^2)^2]\}^{1/2}$.

1. Intensity data were measured by using $\theta-2\theta$ scans. Three standard reflections were monitored every 97 reflections, during data collection, and showed less than 3% variation and no decay. For **1** and **2**, Lorentz, polarization, and ψ-scan absorption corrections were applied by using Crystal Logic software. The following are further experimental crystallographic details: for **1**, $2\theta_{max}$=50°; scan speed 2.0°/min; scan range 2.4 + $\alpha_1\alpha_2$ separation; reflections collected/unique/used, 1948/1865 (Rint = 0.0109)/1865; 182 parameters refined; $(\Delta/\sigma)_{max}$ = 0.090; $(\Delta\rho)_{max}/(\Delta\rho)_{min}$ = 0.605/−0.446 e/Å^3; R1/wR2 (for all data), 0.0318/0.0778; for **2**, $2\theta_{max}$=124°; scan speed 3.0°/min; scan range 2.5 + $\alpha_1\alpha_2$ separation; reflections collected/unique/used, 3555/3397 (Rint = 0.0392)/3329; 383 parameters refined; $(\Delta/\sigma)_{max}$ = 0.162; $(\Delta\rho)_{max}/(\Delta\rho)_{min}$ = 0.700/−0.713 e/Å^3; R1/wR2 (for all data), 0.0687/0.1756; for **3**, $2\theta_{max}$=50°; scan speed 4.2°/min; scan range 2.3+$\alpha_1\alpha_2$ separation; reflections collected/unique/used, 1665/1562 (Rint = 0.0230)/1562; 160 parameters refined; $(\Delta/\sigma)_{max}$ = 0.005; $(\Delta\rho)_{max}/(\Delta\rho)_{min}$ = 0.380/−0.345 e/Å^3; R1/wR2 (for all data), 0.0302/0.0768.

The structures of complexes **1**−**3** were solved by direct methods using SHELXS-86[14] and refined by full-matrix least-squares techniques on F^2 with SHELXL-93.[15] All non-H atoms in the structures of **1**−**3** were refined anisotropically. All H-atoms in the structures of **1** and **3** were located by difference maps and were refined isotropically. In the structure of **2**, all of the H-atoms of the malate ligand and most of the hydrogen atoms belonging to the ammonium counterions and the lattice water molecules were located by difference maps and were refined isotropically. Unfortunately, the missing protons forced us to distinguish NH_4^+ and H_2O molecules on the basis of both temperature factors and hydrogen-bonding distances.

Results

Syntheses. The methodology for the syntheses of the title compounds was based on the initial reaction of simple reagents, in water, at pH ∼8 (for **1** and **2**), and ∼6 (for **3**). In all cases, VCl_3 was chosen as a convenient starting material and it reacted with malic acid, in water, at the stoichiometric molar ratio of 1:1. The pH of the solution was critical for the outcome of the reactions run, following overnight stirring of the initial reaction mixture. On the following day, blue solutions arose with final pH ∼6−7 for **1** and **2**, and pH ∼4.5 for **3**, which were indicative of the presence of vanadium(IV). Specifically, examination of the UV/vis spectra of the derived solutions showed absorptions, in the visible range, that were consistent with the presence of species containing vanadyl moieties (vide infra). Further confirmation of the vanadyl presence in the arisen species, in solution, was provided by EPR spectroscopy (vide infra). Overall, it was shown that, under the employed experimental conditions, vanadium was oxidized to vanadium(IV), thus furnishing intermediate species capable of further reacting with hydrogen peroxide to ultimately yield the vanadium(V)−peroxo−malate complexes **1**−**3**.

Both KOH and ammonia were used effectively to establish the pH of the solution, at which further reactions with H_2O_2 ensued. Use of the above reagents, however, was not invoked only for the mere reason of adjusting the pH of the reaction solution. The employed bases also provided the necessary cations to counterbalance the charge of the anionic complexes generated and subsequently isolated. Addition of H_2O_2 to the blue solutions, derived in all reactions run and at different pH values, gave rise to V^V−malate−peroxo complexes. The overall reactions leading to compounds **1**−**3** are depicted schematically below.

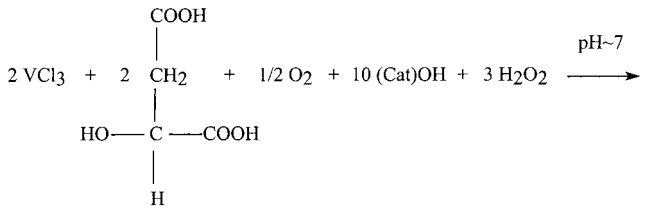

Cat = K^+ ; x = 4 ; y = 7 (**1**)

Cat = NH_4^+ ; x = 3 ; y = 8 (**2**) (Reaction 1)

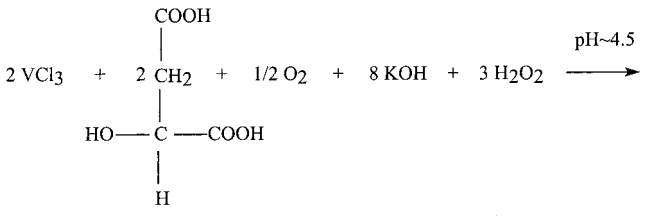

(Reaction 2)

Thus, in all three complexes synthesized, oxidation of vanadium(III) to vanadium(V) took place. Precipitation of the

(14) Sheldrick, G. M SHELXS-86: Structure Solving Program; University of Göttingen, Germany, 1986.
(15) Sheldrick, G. M SHELXL-93: Structure Refinement Program; University of Göttingen, Germany, 1993.

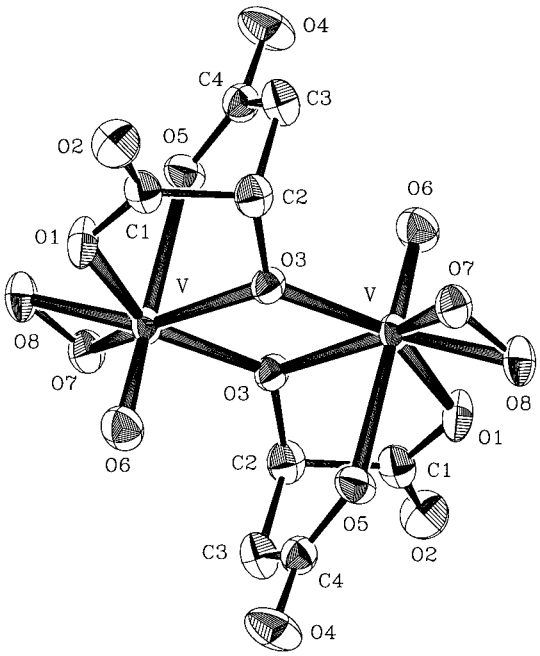

Figure 1. Structure of the $[V_2O_2(O_2)_2(C_4H_3O_5)_2]^{4-}$ anion in **1**, along with the atom labeling scheme. Thermal ellipsoids were drawn by ORTEP and represent 50% probability surfaces.

products out of solution, in crystalline form, was achieved by addition of ethanol at 4 °C. Elemental analyses on the isolated crystalline materials suggested the formulation $K_4[V_2O_2(O_2)_2(C_4H_3O_5)_2]\cdot 4H_2O$, $(NH_4)_4[V_2O_2(O_2)_2(C_4H_3O_5)_2]\cdot 3H_2O$, and $K_2[V_2O_2(O_2)_2(C_4H_4O_5)_2]\cdot 2H_2O$ for **1**, **2**, and **3**, respectively. Of the three materials, **1** appears to be stable in the solid state for 4 days. The other two materials appear to be stable in the open air for longer periods of time (>20 days) with no visible deterioration. Complexes **1** and **2** are insoluble in alcohols (CH_3OH, *i*-PrOH, etc.), acetonitrile, and dimethyl sulfoxide (DMSO), but they dissolve readily in water. Compound **3** is insoluble in organic solvents, like alcohols (CH_3OH, C_2H_5OH, etc.), acetone, and CH_3CN. It dissolves readily in water and, under mild heating, in strongly polar solvents, such as dimethylformamide (DMF) and (DMSO).

X-ray Crystallographic Structures. (a) $K_4[V_2O_2(O_2)_2(C_4H_3O_5)_2]\cdot 4H_2O$ (1) and $(NH_4)_4[V_2O_2(O_2)_2(C_4H_3O_5)_2]\cdot 3H_2O$ (2). The X-ray crystal structures of **1** and **2** consist of discrete anions and cations. Compound **2** crystallizes in the triclinic system $P\bar{1}$ with two molecules per asymmetric unit (heretofore referred to as **2**A and **2**B). Djordjevic and co-workers[16] have previously reported the crystal structure of $(NH_4)_2[VO(O_2)(C_4H_4O_5)]_2\cdot 2H_2O$ (**4**), the only other vanadium−malate−peroxo complex known, which proved to be isostructural to **2**. In the title of the corresponding paper, and throughout the text, they formulated compound **4** as shown above. It is clear, however, from their Table 2 that their proposed formula is $(NH_4)_2[VO(O_2)(C_4H_4O_5)]_2\cdot 3H_2O\cdot 2H_3O$, containing two oxonium cations, a rather strange deduction for that synthesis. On the basis of our structural analysis, we believe that **2** represents the correct formulation. The structure of the anion is the same in both complexes **1** and **2**. Consequently, the two structures will be discussed together. The ORTEP diagram of the anion in **1** is shown in Figure 1. Selected interatomic distances and bond angles for **1** and **2** are listed in Table 2. The anion in both **1** and **2** is a dimer of two vanadium ions with two malate ligands.

Table 2. Selected Bond Distances (Å) and Angles (deg) for **1**, **2**, and **3**

	1	**2**	**3**
V−O(1)	2.064(2)	2.034(3)	2.033(2)
V−O(3)	2.005(2)	1.987(3)	1.986(2)
V−O(3′)	2.025(2)	2.026(3)	2.021(2)
V−O(5)	2.248(2)	2.294(3)	
V−O(6)	1.606(2)	1.599(3)	1.591(2)
V−O(7)	1.874(2)	1.859(3)	1.871(2)
V−O(8)	1.868(2)	1.887(3)	1.869(2)
V(2)−O(16)		1.599(3)	
V(2)−O(17)		1.876(3)	
V(2)−O(18)		1.877(4)	
V(2)−O(13)		2.007(3)	
V(2)−O(13″)		2.035(3)	
V(2)−O(11)		2.042(4)	
V(2)−O(15)		2.257(3)	
O(6)−V−O(8)	102.2(1)	100.2(2)	101.85(9)
O(6)−V−O(7)	101.2(1)	101.5(2)	103.9(1)
O(8)−V−O(7)	44.90(9)	44.8(2)	45.10(8)
O(6)−V−O(3)	96.65(9)	98.3(2)	102.35(9)
O(8)−V−O(3)	151.37(9)	151.9(2)	147.06(8)
O(7)−V−O(3)	149.96(8)	148.7(1)	144.75(8)
O(6)−V−O(3′)	97.6(1)	97.9(2)	97.86(9)
O(8)−V−O(3′)	125.29(8)	126.0(2)	126.43(9)
O(7)−V−O(3′)	81.51(8)	81.8(1)	81.97(9)
O(3)−V−O(3′)	72.30(8)	71.6(2)	71.43(9)
O(6)−V−O(1)	91.2(1)	92.9(2)	93.01(9)
O(8)−V−O(1)	80.86(8)	79.9(2)	79.3(1)
O(7)−V−O(1)	125.69(8)	124.3(1)	123.9(1)
O(3)−V−O(1)	77.38(7)	78.2(1)	77.42(9)
O(3′)−V−O(1)	149.17(7)	149.0(1)	148.52(7)
O(6)−V−O(5)	172.73(9)	173.1(2)	
O(8)−V−O(5)	81.44(8)	81.7(1)	
O(7)−V−O(5)	85.80(8)	84.5(1)	
O(3)−V−O(5)	77.71(7)	77.6(1)	
O(3′)−V−O(5)	85.12(8)	86.1(1)	
O(1)−V−O(5)	83.13(9)	80.9(1)	

[a] Symmetry transformations used to generate equivalent atoms: (1) ′ $-x, -y, -z+1$; (2) ′ $-x+1, -y+2, -z+1$; ″ $-x, -y, -z$; (3) ′ $-x, -y, -z$.

The core of the dimeric structure consists of a rhombic $V^V{}_2O_2$ unit, with the two vanadium ions, in the 5+ oxidation state, bridged by the alkoxide oxygens of the coordinated malates. The anion $[V_2O_2(O_2)_2(C_4H_3O_5)_2]^{4-}$ sits on a crystallographic inversion center. Therefore, the V_2O_2 core is planar and defines the plane around which the ligands are appropriately arranged. The malate ligand is triply deprotonated. As such, it provides both its carboxylate and hydroxyl groups for tridentate coordination to the two metal ions. The coordination environment around each vanadium can be described as a distorted pentagonal bipyramid. The equatorial plane of the bipyramid is comprised of atoms O(1), O(3), O(3′), O(7), and O(8). The latter two belong to the peroxo group O−O coordinated to V^V. The axial positions are occupied by the atoms O(5), belonging to the carboxylate group of the malate ligand attached to vanadium, and O(6), belonging to the oxo group doubly bonded to the same metal. Structural comparisons of the bond distances and angles in **1** and **2** with corresponding distances and angles in other vanadium(V)-containing species[16−21] are given in Table 3.

(16) Djordjevic, C.; Lee-Renslo, M.; Sinn, E. *Inorg. Chim. Acta* **1995**, *233*, 97−102.
(17) Djordjevic, C.; Lee, M.; Sinn, E. *Inorg. Chem.* **1989**, *28*, 719−723.
(18) Süss-Fink, G.; Stanislas, S.; Shul'pin, G. B.; Nizova, G. V.; Stoeckli-Evans, H.; Neels, A.; Bobillier, C.; Claude, S. *J. Chem. Soc., Dalton Trans.* **1999**, 3169−3175.
(19) Wei, Y.-G.; Zhang, S.-W.; Huang, G.-Q.; Shao, M.-C. *Polyhedron* **1994**, *13*, 1587−1591.
(20) Drew, R. E.; Einstein, F. W. B. *Inorg. Chem.* **1973**, *12*, 829−835.
(21) Szentivanyi, H.; Stomberg, R. *Acta Chem. Scand.* **1983**, *A37*, 709−714.

Table 3. Bond Distances (Å) and Angles (deg) in [$VO(O_2)$]-Containing Compounds

compound	distances (Å)			angles (deg)	
	V=O	V−O	O−O	$(O-V-O)_{equatorial}$[h]	$(O-V-O)_{apical}$[i]
$K_4[V_2O_2(O_2)_2(C_4H_3O_5)_2]\cdot 4H_2O$ (**1**)[a]	1.606(2)	1.868(2)−2.248(2)	1.429(3)	44.90(9)−81.51(9)	77.71(7)−102.2(1)
$(NH_4)_4[V_2O_2(O_2)_2(C_4H_3O_5)_2]\cdot 3H_2O$ (**2**)[a]	1.599(3)	1.859(3)−2.294(3)	1.428(5)	44.8(2)−81.8(1)	77.6(1)−101.5(2)
$(NH_4)_2[VO(O_2)(C_4H_4O_5)]_2\cdot 2H_2O$[16]	1.601(1)−1.603(1)	1.874(1)−2.270(1)	1.442(2)	45.12(6)−81.60(5)	77.41(4)−102.12(6)
$K_2[VO(O_2)(C_6H_6O_7)]_2\cdot 2H_2O$[b,17]	1.601(1)	1.873(1)−2.039(1)	1.427(2)	44.61(6)−83.73(5)	73.02(5)−104.19(6)
$(NH_4)[VO(O_2)(C_5H_3N_2O_2)_2]\cdot 2H_2O$[c,18]	1.598(1)	1.863(1)−2.189(1)	1.412(2)	44.18(6)−79.81(5)[k]	75.08(5)−104.20(6)[k]
$K_2[VO(O_2)(C_6H_6NO_6)]$[d,19]	1.607(3)	1.874(4)−2.043(4)	1.431(4)	44.8(2)−80.2(2)[k]	77.3(1)−106.4(2)[k]
$(NH_4)[VO(O_2)(H_2O)(C_5H_3N(COO)_2)]\cdot x H_2O$[e,20]	1.579(2)	1.870(2)−2.211(2)	1.441(3)	45.3(3)−81.6(1)[k]	80.0(1)−102.3(1)[k]
$[VO(O_2)(C_5H_4NCOO)(C_{10}H_8N_2)]\cdot H_2O$[f,g,21]	1.604(5)	1.862(5)−2.270(6)	1.424(7)	44.7(2)−79.2(2)[k]	73.9(2)−102.6(2)[k]
$K_2[V_2O_2(O_2)_2(C_4H_4O_5)_2]\cdot 2H_2O$ (**3**)[a]	1.591(2)	1.869(2)−2.033(2)	1.434(3)	45.10(8)−71.43(9)	93.01(9)−103.9(1)
$K_2[\{VO(O_2)(L\text{-}tartH_2)\}_2(\mu\text{-}H_2O)]\cdot 5H_2O$[22]	1.584(6)−1.588(5)	1.861(5)−2.015(5)	1.423(7)−1.444(7)	44.5(2)−84.3(2)	72.0(2)−102.5(3)
$(Bu_4N)_2[V_2O_2(O_2)_2(L\text{-}lact)_2]\cdot 2H_2O$[23]	1.600(5)−1.605(6)	1.830(8)−2.049(6)	1.232(11)−1.433(9)	42.1(3)−124.9(3)	94.5(4)−119.2(3)

[a] This work. [b] $C_6H_6O_7^{2-}$ = citrate. [c] $C_5H_3N_2O_2^-$ = pyrazine-2-carboxylate. [d] $C_6H_6NO_6^{3-}$ = nitrilotriacetate. [e] $C_5H_3N(COO)_2^{2-}$ = pyridine-2,6-dicarboxylate. [f] $C_5H_4NCOO^-$ = pyridine-2-carboxylate. [g] $C_{10}H_8N_2$ = 2,2′-bipyridine. [h] O−V−O angle range in the equatorial plane. [i] O−V−O angles between the axial and equatorial ligands. [k] Includes O−V−N angles in the equatorial plane.

Table 4. Hydrogen-Bonding Interactions for Compounds **1**−**3**

interaction	D···A (Å)	H···A (Å)	D−H···A (deg)	symmetry transformation
		Compound **1**		
OW1−HW1A···O1′	2.879	2.086	171.7	$-1+x, y, z$
OW1−HW1B···O4′	2.711	1.894	168.9	$-1-x, 0.5+y, 0.5-z$
OW2−HW2B···O3′	3.008	2.357	146.0	$-x, -y, 1-z$
		Compound **2**		
N1−HN1A···O4′	2.933	2.124	169.7	$1+x, y, z$
N1−HN1B···O8′	2.953	1.950	165.9	$1-x, 1-y, 1-z$
N1−HN1C···O15′	3.092	2.169	157.2	$1-x, 1-y, 1-z$
N1−HN1D···O2′	2.771	1.832	165.3	x, y, z
N2−HN2A···O12′	2.802	1.815	165.6	x, y, z
N2−HN2B···O13′	3.042	2.303	149.6	$1-x, -y, -z$
N2−HN2C···O4′	2.861	2.182	172.2	$1-x, 1-y, 1-z$[a]
N3−HN3A···O7′	2.787	2.166	167.5	x, y, z
N3−HN3B···W3′	2.768	2.017	162.1	x, y, z[b]
N4−HN4A···W2′	2.969	2.091	151.2	$1-x, 1-y, -z$[c]
W1−HW1A···O14′	2.693	1.734	138.0	$1+x, 1-y, z$[d]
W2−HW2A···W1′	2.730	2.124	129.9	x, y, z
W2−HW2B···O11′	2.786	1.881	173.3	x, y, z
W3−HW3A···O14′	2.692	2.105	134.0	$-x, 1-y, 1-z$
W3−HW3B···O3′	3.307	2.267	157.6	$1-x, 2-y, 1-z$
		Compound **3**		
O4−HO4···O2′	2.576	1.877	176.3	$x, -0.5-y, 0.5+z$
OW−HWB···OW′	2.965	2.439	173.4	$1-x, -y, 1-z$

[a] HN2D was not located. [b] HN3C and HN3D were not found. [c] HN4B, HN4C, and HN4D were not found. [d] HW1B was not located.

The 4− charge, generated on the complex anion, is counterbalanced by four potassium and four ammonium ions in **1** and **2,** respectively. The potassium cations in **1** are in contact with the carboxylate oxygens of the malate anion as well as peroxo, oxo, and lattice water oxygens at distances in the range 2.706−3.023 Å (eight contacts for K1) and 2.674−3.020 Å (six contacts for K2). The presence of water molecules of crystallization in both structures and the ammonium counterions in **2** are responsible for the establishment of an extensive hydrogen-bonding network (Table 4).

(b) $K_2[V_2O_2(O_2)_2(C_4H_4O_5)_2]\cdot 2H_2O$ (3). The compound consists of discrete cations and anions. An ORTEP diagram of the anion in **3** is shown in Figure 2. Selected interatomic distances and bond angles are listed in Table 2. The anions are composed of dimeric V_2O_2 units sitting on a crystallographic inversion center, thus rendering the dimeric core planar and the complex centrosymmetric. The two vanadium ions, in the core, are in the 5+ oxidation state and are surrounded by two malate ligands, which appear to be doubly deprotonated. As such, the two malates each employ one of their terminal carboxylates and the hydroxyl group to coordinate to the two vanadium ions. The other terminal carboxylate groups, which belong to the $-CH_2COO$ end of the malate ligands, are protonated. Due to the protonated nature of those terminal carboxylates, it appears that the latter move away from the vanadium ion(s), giving rise to a pentagonal pyramidal coordination geometry. The base of the pyramid is comprised of the oxygen terminals of the ligands, and the peroxo group, which is introduced into the molecule upon reaction with H_2O_2. The doubly bonded oxygen, attached to the vanadium ion, occupies the axial position of the pyramid. Comparison of the bond distances and angles in **3** with those observed in other vanadium(V)-containing complexes[22,23] are given in Table 3.

The angles formed between the vanadium and the oxygens of the peroxo group, in the VO_2 isosceles triangle defined by the peroxide oxygens and the vanadium ion, appear to be almost

(22) Schwendt, P.; Svancarek, P.; Kuchta, L.; Marek, J. *Polyhedron* **1998**, *17*, 2161−2166.
(23) Schwendt, P.; Svancarek, P.; Smatanova, I.; Marek, J. *J. Inorg. Biochem.* **2000**, *80*, 59−64.

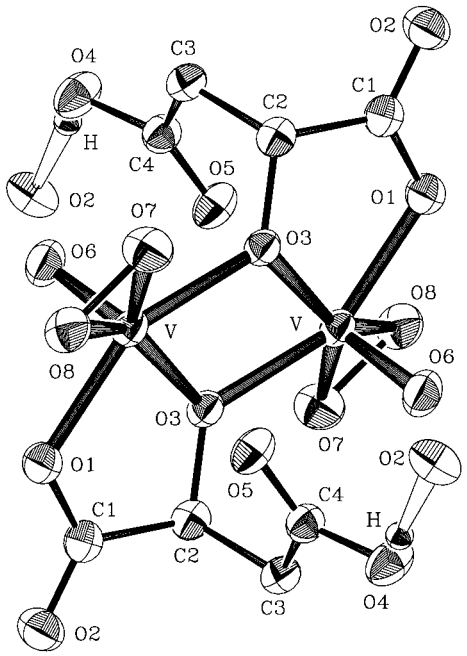

Figure 2. Structure of the $[V_2O_2(O_2)_2(C_4H_4O_5)_2]^{2-}$ anion in **3**, along with the atom labeling scheme. Thermal ellipsoids were drawn by ORTEP and represent 50% probability surfaces.

identical. That picture is in line with observations on the corresponding angles in complex **1**.

Due to the double deprotonation of the two malate ligands bound to the V_2O_2 core, the charge of the resulting complex is reduced by two units, in comparison to the 4− charge on the anion in **1** and **2**. Consequently, the resulting 2− charge is counterbalanced by two potassium ions. The potassium ions are in contact with seven oxygen atoms (2.786−3.099 Å), which reside on the carboxylate groups of the malate ions, the peroxo group, and lattice water molecules.

The protonated terminal carboxylate of the malate ion is strongly hydrogen bonded to the coordinated carboxylate of a neighboring molecule, thus forming polymeric chains [HO(4)···O(2′) = 1.877 Å, O(4)···O(2′) = 2.576 Å, O(4)−HO(4)···O(2) = 176.3°; O(2′): x, $-0.5 - y$, $0.5 + z$]. The water molecules of crystallization are also hydrogen bonded, HWb···OW′ = 2.439 Å, OW···OW′ = 2.965 Å, OW−HWb···OW′ = 173.4° (OW′: $1 - x$, $-y$, $1 - z$) (Table 4).

Electronic Spectroscopy. The UV/vis spectra of the blue aqueous reaction solutions at pH ∼7 and ∼4.5 were recorded in the range 200−1000 nm, in an effort to gain insight into the nature of the intermediate species formed, prior to the addition of hydrogen peroxide. The experiments were carried out at vanadium concentrations in the range 3 mM to 0.1 M. The blue solution at pH ∼7 showed bands at 810 and 601 nm and a shoulder around 415 nm. The blue solution at pH ∼4.5 showed bands at 788 and 603 nm and a shoulder around 410 nm. In both cases, the aforementioned spectral features denoted the presence of d−d transitions characteristic of $\{V{=}O\}^{2+}$-containing species. More specifically, the absorptions in the range 600−850 nm could be attributed[24] to previously proposed transitions $d_{xy} \rightarrow d_{xz},d_{yz}$ [810 nm (pH ∼7), 788 nm (pH ∼4.5)], $d_{xy} \rightarrow d_{x^2-y^2}$ [601 nm (pH ∼7), 603 nm (pH ∼4.5)], and $d_{xy} \rightarrow d_{z^2}$ according to the OSM energy level scheme.[25] It is very likely that the $d_{xy} \rightarrow d_{z^2}$ transition expected in the 500 nm region was hidden, in our case, beneath the broad band at 601 nm. With regard to the high-energy spectral feature around 415 nm (pH ∼7) or 410 nm (pH ∼4.5), it could be tentatively ascribed to a LMCT transition, in accordance with previous observations in the literature.[24,26]

The UV/vis spectrum of **2** in water, at pH ∼7, exhibited a shoulder-like band at 340 nm ($\epsilon \sim 756$ M^{-1} cm^{-1}) and a strong band rising into the UV at 219 nm ($\epsilon = 9990$ M^{-1} cm^{-1}). The absorption observed at 340 nm was attributed to the presence of a peroxo to vanadium ligand to metal charge transfer (LMCT).[27] The spectrum of **3** in water, at pH ∼4.5, also showed a broad band at 422 nm ($\epsilon = 317$ M^{-1} cm^{-1}) and a strong band rising into the UV, with a maximum at 234 nm ($\epsilon = 7203$ M^{-1} cm^{-1}). Here, as well, the band at 422 nm was tentatively attributed to the presence of a peroxo to vanadium LMCT. It appears, therefore, that in the pH range examined here, the peroxo group remains attached to the vanadium ion, as that is indicated by the LMCT absorption at 340 nm in complex **2** and at 422 nm in complex **3**, further supporting the idea of a stable $[(V{=}O)(O_2)]^+$ unit in both classes of complexes. The presence of the weak LMCT band, as surmised by Evans,[28] was also confirmed in the case of a vanadium−peroxo−citrate complex bearing a $[(V{=}O)_2O_2(O_2)_2]^{2-}$ core[17] and was reasonably assigned to a $\pi_v^* \rightarrow$ d transition.[27,28] The intense absorption bands at 219 nm in **2** and 234 nm in **3**, in the ultraviolet region, may be associated with the $\pi_h^* \rightarrow d\sigma^*$ LMCT transition. This transition was proposed to occur at even higher energies than the $\pi_v^* \rightarrow$ d transition, due to the stabilization of the π_h^* σ peroxo to metal bonding orbital. More definitive assignments cannot be made, at this point, due to the lack of in-depth spectroscopic studies.[27,28]

FT-IR Spectroscopy. The FT-infrared spectra of the title compounds, in KBr, exhibited strong absorptions for various vibrationally active groups. Specifically, absorptions for the antisymmetric stretching vibrations $\nu_{as}(COO^-)$ of the carbonyls in the terminal carboxylates appeared between 1639 and 1565 cm^{-1} for **1**, 1639 and 1565 cm^{-1} for **2**, and 1675 and 1577 cm^{-1} for **3**. Symmetric stretching vibrations $\nu_s(COO^-)$ were observed in the range 1425−1380 cm^{-1} for **1**, 1421 and 1380 cm^{-1} for **2**, and 1448−1384 cm^{-1} for **3**. The carbonyl frequencies for the aforementioned stretches appeared to be shifted to lower values compared to those of free malic acid, indicating changes in the vibrational status of the ligand upon coordination to the vanadium ion.[17,29] In all of the compounds studied here, the difference between the symmetric and antisymmetric stretches, $\Delta(\nu_{as}(COO^-) - \nu_s(COO^-))$, was on the order of 200 cm^{-1}, indicating that the carboxylate groups in the molecules were either free or coordinated to vanadium in a monodentate fashion.[29] The latter deduction was in agreement with the observed X-ray crystal structures of **1**−**3**. The aforementioned tentative assignments were also in consonance with previous results reported for carboxylic acid complexes of various metals.[30] The V=O vibrations were assigned to bands appearing at 954 cm^{-1} for **1** and **2**, and 976 cm^{-1} for **3**. The

(24) Selbin, J.; Morpurgo, L. *J. Inorg. Nucl. Chem.* **1965**, *27*, 673−678.
(25) Ortolano, T. R.; Selbin, J.; McGlynn, S. P. *J. Chem. Phys.* **1964**, *41*, 262−268.
(26) Micera, G.; Dessi, A. *J. Inorg. Biochem.* **1988**, *33*, 99−109.
(27) (a) Lever, A. B. P.; Gray, H. B. *Inorg. Chem.* **1980**, *19*, 1823−1824. (b) Lever, A. B. P.; Gray, H. B. *Acc. Chem. Res.* **1978**, *11*, 348−355.
(28) Evans, D. F. *J. Chem. Soc.* **1957**, 4013−4018.
(29) Deacon, G. B.; Philips, R. *J. Coord. Chem. Rev.* **1980**, *33*, 227−250.
(30) (a) Matzapetakis, M.; Raptopoulou, C. P.; Terzis, A.; Lakatos, A.; Kiss, T.; Salifoglou, A. *Inorg. Chem.* **1999**, *38*, 618−619. (b) Matzapetakis, M.; Raptopoulou, C. P.; Tsohos, A.; Papefthymiou, B.; Moon, N.; Salifoglou, A. *J. Am. Chem. Soc.* **1998**, *50*, 13266−13267. (c) Tsaramyrsi, M.; Kaliva, M.; Raptopoulou, C. P.; Tangoulis, V.; Terzis, A.; Giapintzakis, J.; Salifoglou, A., submitted for publication.

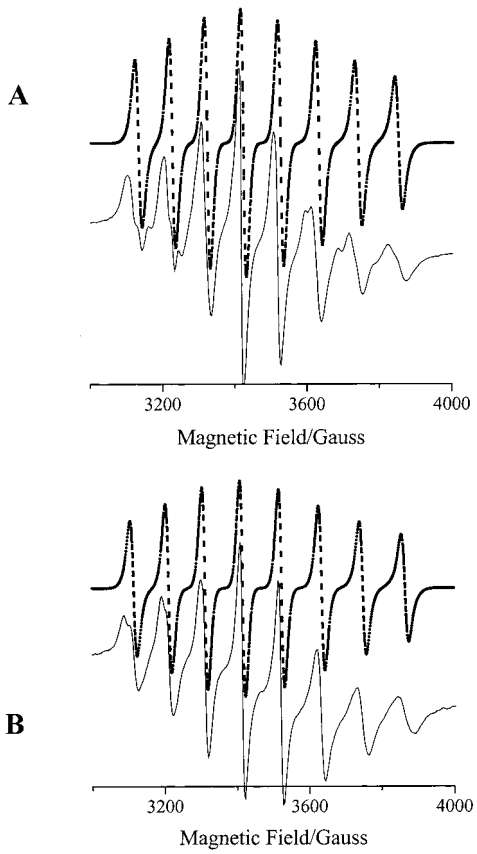

Figure 3. (A) X-band EPR spectrum of the intermediate blue solution derived from the reaction leading to the synthesis of **1** at pH ∼7, at room temperature. (B) X-band EPR spectrum of the intermediate blue solution derived from the reaction leading to the synthesis of **3** at pH ∼4.5, at room temperature. The dotted lines represent the fitting of the actual spectra.

peroxo ν(O−O) stretches were assigned to vibrations at 926 cm^{-1} for **1** and **2**, and 921 cm^{-1} for **3**. Both of the above group assignments were in line with corresponding assignments previously reported for various vanadium(V)−peroxo species.[10,17,19,31,32]

EPR Spectroscopy. The X-band solution EPR spectra of the intermediate blue solutions, at vanadium concentrations in the range 40 μM to 0.1 M, derived from the reactions targeting complexes **1**−**3**, were recorded at room temperature and at 4 K. The spectra for both pH ∼7 and ∼4.5 solutions at room temperature (Figure 3) clearly showed the presence of eight lines, typical of vanadium(IV) ($I = 7/2$) in vanadyl ($V{=}O^{2+}$) containing species. More specifically, in the case of the pH ∼7 solution, the spectrum exhibited signals with isotropic parameters $g_{iso} = 1.96$ and $A_{iso} = 94 \times 10^{-4}$ cm^{-1}. In the case of the pH ∼4.5 blue solution, the spectrum exhibited signals with isotropic parameters $g_{iso} = 1.96$ and $A_{iso} = 98 \times 10^{-4}$ cm^{-1}. The aforementioned values were close to those that had previously been reported in the literature.[26] Moreover, the spectra of the blue solutions for the two different pH values at 4 K (Figure 4) showed a weak signal at $g = 4.0$, which corresponds to a half-field transition, revealing the small ferromagnetic character ($S = 1$) of an interaction between two V^{IV} ions. Overall, the spectra of both solutions were consistent with the presence of dimeric species in solution, containing vanadyl ($V{=}O^{2+}$)

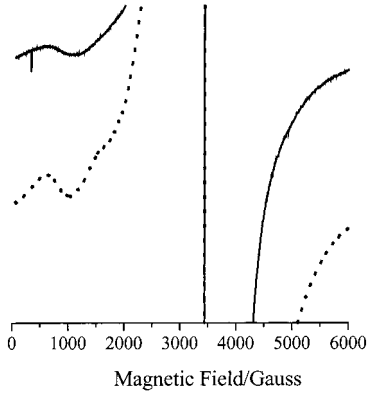

Figure 4. X-band EPR spectrum of the intermediate blue solution derived from the reaction leading to the synthesis of **1** at pH ∼7, at 4 K. The spectrum is focused on the low-field region, showing the presence of the half-field transition, which reflects the weak ferromagnetic interaction between two vanadium(IV) ions.

moieties bridged by the malate hydroxyl oxygens. Taking into consideration the fact that the isotropic coupling constants, derived from the spectroscopic data, reflect the equatorial ligand environment in the complexes emerging in solution, an attempt was made to predict which possible ligands might be present around the vanadyl moieties of the $VO(O_4)$ systems at the two pH values. On the basis of the additivity relationship[33]

$$A_{0,\mathrm{calc}} = \sum_i n_i A_{0,i/4}$$

where n_i is the number of different donor groups L_i in the equatorial plane, and $A_{0,i}$ is the experimental isotropic coupling constant for a complex with all four donor groups the same:

(a) The $A_{0,\mathrm{calc}}$ for a complex with equatorial ligands of the type R−COO^-, R−O^-, and H_2O, in the blue solution at pH ∼7 was 93×10^{-4} cm^{-1} compared to the value of 94×10^{-4} cm^{-1} derived from the experimental data. A tentative model consistent with the derived EPR data is shown below.

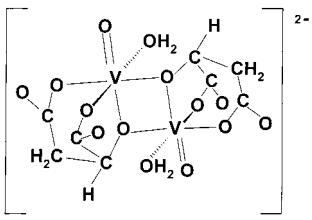

(b) The $A_{0,\mathrm{calc}}$ for a complex with equatorial ligands of the type R−COO^-, R−O^-, and H_2O, in the blue solution at pH ∼4.5 was 95×10^{-4} cm^{-1} compared to the value of 98×10^{-4} cm^{-1} derived from the experimental data. A tentative model consistent with the derived EPR data is shown below.

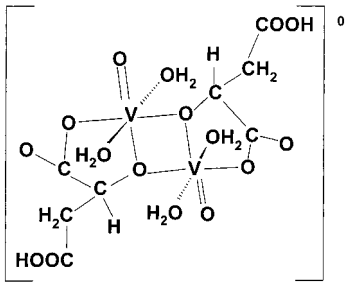

Dimeric complexes containing vanadyl moieties and prescribing to the properties emerging from the present EPR data have been seen before for the tricarboxylic acid citrate.[34]

(31) Griffith, W. P.; Wickins, T. D. *J. Chem. Soc. A* **1968**, 397−400.
(32) Vuletic, N.; Djordjevic, C. *J. Chem. Soc., Dalton Trans.* **1973**, 1137−1141.

Discussion

The expedient syntheses, isolation from aqueous solutions, and structural characterization of complexes **1**−**3** revealed the extent of diversity in the oxidative chemistry of vanadium(III) with malic acid and hydrogen peroxide, as a function of the pH in the aqueous media employed. Outstanding among the features unravelled by the X-ray structures of the title complexes were the following:

(a) The coordination geometry around vanadium(V), which changes from pentagonal bipyramidal to pentagonal pyramidal, in going from pH ∼7 to ∼4.5. That reduction in the coordination number is consistent with the inability of the protonated terminal carboxylate of the malate ligand to bind vanadium.

(b) The protonation state of the malate ligand, which changes from the fully, triply deprotonated state in **1** and **2**, at pH ∼7, to the doubly deprotonated state in **3**, at pH ∼4.5.

(c) The charge of the complexes, which changes from 4− in **1** and **2**, at pH ∼7, to 2- in **3**, at pH ∼4.5, thus denoting the consequences of protonation of the malate ligand attached to the V_2O_2 core.

In all of the above cases of complex anions **1**−**3**, the structural and electronic components that remained intact included (a) the planar $V^V{}_2O_2$ core of the title complexes, (b) the 5+ oxidation state of vanadium, (c) the peroxide moiety coordinated to vanadium, and (d) the V═O units, and their anti-conformation in all three complexes. Some or all of the aforementioned features could conceivably be key factors in determining any potential biological activity, which synthetic vanadium(V)-peroxo complexes might promote[9,12,35]

A number of solution speciation studies on vanadium polycarboxylate systems were carried out in the past, with the help of potentiometric and various NMR methods. Such systems included, among others, citrate[36] (a structural cognate of malic acid) and malate,[37] as potential vanadium multidentate binders in the absence of H_2O_2. In the vanadium(V)−citrate system, the studies supported the existence of $V^V{}_2O_2$ dimeric cores. Subsequent synthetic studies confirmed that contention and proved the presence of the dimeric $V^V{}_2O_2$ cores in the presence[17] and absence[18] of peroxo groups. In the case of the aqueous vanadium(V)−malate system, the presence of complexes with a vanadium:malate composition of *n*:*n* was proposed, thus not discounting the likely existence of dimeric $V^V{}_2O_2$ species similar to those referred to above ($n = 2$). Finally, very recently, speciation studies on the vanadium(V)−peroxide complexes, in the presence of L-lactic acid, suggested the presence of dimeric species similar to the aforementioned, in solution and in the pH range 2−7.[38] Our EPR and UV/vis investigations into the nature of the intermediate species forming during the syntheses of complexes **1**−**3** suggested the presence of similar $V^{IV}{}_2O_2$ core containing dimeric species in solution. These species underwent further oxidation by H_2O_2 to yield $V_2{}^V{-}O_2$ core-containing species, with concurrent coordination of the peroxo group to the oxidized vanadium ions. These observations confirmed the robustness of the core in two oxidation states, with the one bearing vanadium(V) especially akin to peroxo coordination chemistry. Furthermore, the above solution chemistry appeared to be in line with the final solid-state structures described in this work. In view of the fact, however, that no solution speciation studies exist to date, on either vanadium−citrate− or vanadium−malate−peroxo ternary systems, *care should be exercised in projecting the presence of such peroxo species from the solid state to the solution state*. Consequently, taking into consideration the data on complexes **1**−**3**, specifically the structural similarity of their central $V^V{}_2O_2$ units to those (a) reported in the crystallographically characterized complexes of citrate, tartrate,[22] lactate,[23] and (b) suggested by solution studies,[38] it would not be unreasonable to propose that similar peroxovanadium complexes with malic acid might exist in physiologically relevant media. Such a contention, however, should await firm chemical confirmation (potentiometry, ^{51}V NMR, etc.).

Overall, the chemistry studied here may reflect similar chemistry carried out by vanadium(III-V) in the presence of carboxylic substrates/ligands in biological fluids under variable pH conditions. From that point of view, the unravelling of structural and physicochemical properties of complexes, analogous to those arisen from this work, will undoubtedly contribute to the further understanding of the chemical reactivity of vanadium(III-V) in biologically related media containing dicarboxylates, like malate. Synthetic strategies targeting such species and efforts to characterize them are currently pursued in our laboratory.

Acknowledgment. This work was supported with funds provided by the Department of Chemistry, University of Crete, Greece (Grant by ELKE No. 1186). We are also grateful to the Agricultural Bank of Greece and Mrs. Athina Athanasiou for providing financial support to C. P. R. and A.T.

Supporting Information Available: X-ray crystal crystallographic files, in CIF format, and listings of positional and thermal parameters and H-bond distances and angles for **1**−**3**. The material is available free of charge via Internet at http://pubs.acs.org.

IC000894O

(33) Chasteen, N. D. In *Biological Magentic Resonance*; Berliner, L. J., Reuben, J., Eds.; Plenum Press: New York, 1981; Vol. 3, pp 53−119.

(34) Velayutham, M.; Varghese B.; Subramanian, S. *Inorg. Chem.* **1998**, *37*, 1336−1340.

(35) (a) Shaver, A.; Ng, J. B.; Hall, D. A.; Posner, B. I. *Mol. Cell Biochem.* **1995**, *153*, 5−15. (b) Bevan, A. P.; Drake, P. G.; Yale, J. F.; Shaver, A.; Posner, B. I. *Mol. Cell Biochem.* **1995**, *153*, 49−58. (c) Yale, J. F.; Lachance, D.; Bevan, A. P.; Vigeant, C.; Shaver, A.; Posner, B. I. *Diabetes* **1995**, *44*, 1274−1279.

(36) Ehde, P. M.; Andersson, I.; Pettersson, L. *Acta Chem. Scand.* **1989**, *43*, 136−143.

(37) (a) Caldeira, M. M.; Ramos, M. L.; Oliveira, N. C.; Gil, V. M. S. *Can. J. Chem.* **1987**, *65*, 2434−2440. (b) Preuss, F.; Rosenhahn, L. J. *Inorg. Nucl. Chem.* **1972**, *34*, 1691−1703.

(38) Justino, L. L. G.; Ramos, M. L.; Caldeira, M. M.; Gil, V. M. S. *Eur. J. Inorg. Chem.* **2000**, 1617−1621.